Manuscript submitted to
AIMS' Journals
Volume **X**, Number **0X**, XX **200X**

doi:10.3934/xx.xxxxxxx

pp. **X–XX**

arXiv:2001.09187v4 [math.NA] 12 Nov 2020

CERTIFIED AND FAST COMPUTATIONS WITH SHALLOW COVARIANCE KERNELS

Daniel Kressner

MATH-ANCHP, École Polytechnique fédérale de Lausanne
1015 Lausanne, Switzerland

Jonas Latz*

Department of Applied Mathematics and Theoretical Physics, University of Cambridge
Cambridge CB3 0WA, United Kingdom

Stefano Massei

Department of Mathematics and Computer Science, Eindhoven University of Technology
5612 AZ Eindhoven, Netherlands

Elisabeth Ullmann

Department of Mathematics, Technical University of Munich
85748 Garching, Germany

(Communicated by the associate editor name)

Abstract. Many techniques for data science and uncertainty quantification demand efficient tools to handle Gaussian random fields, which are defined in terms of their mean functions and covariance operators. Recently, parameterized Gaussian random fields have gained increased attention, due to their higher degree of flexibility. However, especially if the random field is parameterized through its covariance operator, classical random field discretization techniques fail or become inefficient. In this work we introduce and analyze a new and certified algorithm for the low-rank approximation of a parameterized family of covariance operators which represents an extension of the *adaptive cross approximation* method for symmetric positive definite matrices. The algorithm relies on an affine linear expansion of the covariance operator with respect to the parameters, which needs to be computed in a preprocessing step using, e.g., the empirical interpolation method. We discuss and test our new approach for isotropic covariance kernels, such as Matérn kernels. The numerical results demonstrate the advantages of our approach in terms of computational time and confirm that the proposed algorithm provides the basis of a fast sampling procedure for parameter dependent Gaussian random fields.

2020 *Mathematics Subject Classification.* 62M40 65R20 65C20 65D15 65G20 .

Key words and phrases. Adaptive cross approximation, covariance matrix, greedy algorithm, Wasserstein distance, Gaussian random field.

Jonas Latz and Elisabeth Ullmann acknowledge the support by Deutsche Forschungsgemeinschaft (DFG) and Technische Universität München (TUM) through the TUM International Graduate School of Science and Engineering (IGSSE) within the project 10.02 BAYES. The work of Stefano Massei has been supported by the SNSF research project *Fast algorithms from low-rank updates*; grant number: 200020_178806.

* Corresponding author: Jonas Latz.

1. **Introduction.** Deep neural networks (DNNs) play a fundamental role in modern machine learning and artificial intelligence, see [25] for an overview. They are an example for a *deep model*, which is constructed by composing a number of mathematical models ('layers'). By this construction, deep models allow for much more flexibility in data-driven applications than offered by a standard model. The *layers* in deep models are often rather simple, like artificial neurons in DNNs or linear functions. Hence, the computational cost when *training* a DNN is caused by a large number of layers, not by the complexity of the single models. In other situations, however, the layers themselves are highly complex. Here, already the training of a *shallow model* – consisting of few layers – may require an immense computational cost.

In this article, we consider a specific shallow model with two layers. The outer layer is a Gaussian process on a compact domain with a covariance kernel containing unknown parameters. The inner layer is a probability measure that describes the distribution of the unknown parameters in the covariance kernel. We (and, e.g., [14]) refer to such a shallow model as a *shallow Gaussian process* in contrast to *deep Gaussian processes* that recently gained popularity in the literature; see [7, 9, 11]. Shallow Gaussian processes appear especially in the uncertainty quantification literature, see [10, 29, 32, 38, 45], where they are used to model random, function-valued inputs to partial differential equations. Additionally, they are applicable in a variety of statistical or machine learning tasks; see, e.g., [22] and Chapter 5 of [34].

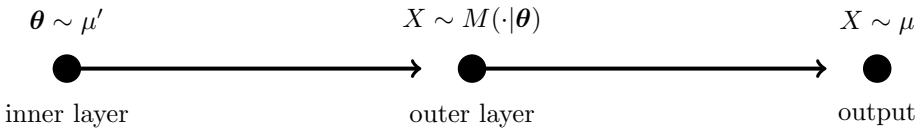


FIGURE 1. Illustration of a shallow Gaussian process. On the inner layer, a random variable $\boldsymbol{\theta}$ with law μ' is sampled. On the outer layer, the process $X \sim M(\cdot|\boldsymbol{\theta})$ is sampled. Then, X follows the distribution of the shallow Gaussian process μ.

In practice, the Gaussian process on the outer layer is discretized with a very large number of degrees of freedom $n \in \mathbb{N}$. The discretization induces a parameterized Gaussian measure on $(\mathbb{R}^n, \mathcal{B}\mathbb{R}^n)$ of the form

$$M(\cdot|\boldsymbol{\theta}) := \mathrm{N}(\mathbf{m}(\boldsymbol{\theta}), \mathbf{C}(\boldsymbol{\theta})) \qquad (\boldsymbol{\theta} \in \Theta).$$

Here $\boldsymbol{\theta}$ refers to the unknown parameters that are contained in the parameter space Θ, which is associated with some σ-algebra $\mathcal{A}$. Moreover, $\mathbf{m} : \Theta \to \mathbb{R}^n$ is a measurable function and $\mathbf{C} : \Theta \to \mathrm{SPSD}(n)$ is a measurable function mapping parameters $\boldsymbol{\theta} \in \Theta$ to the set of *symmetric positive semidefinite* (SPSD) matrices in $\mathbb{R}^{n\times n}$. By this assumption, M is a Markov kernel mapping from $(\Theta, \mathcal{A})$ to $(\mathbb{R}^n, \mathcal{B}\mathbb{R}^n)$.

The inner layer is represented by a probability measure μ' on $(\Theta, \mathcal{A})$. The shallow Gaussian process is then defined as the composition of μ' and M:

$$\mu := \mu' M := \int_\Theta M(\cdot|\theta)\mu'(\mathrm{d}\boldsymbol{\theta}) = \int_\Theta \mathrm{N}(\mathbf{m}(\boldsymbol{\theta}), \mathbf{C}(\boldsymbol{\theta}))\mu'(\mathrm{d}\boldsymbol{\theta}) =: \mu' \mathrm{N}(\mathbf{m}, \mathbf{C});$$

which is a well-defined probability measure on $(\mathbb{R}^n, \mathcal{B}\mathbb{R}^n)$. In Figure 1, we visualize the simple graph structure behind the shallow Gaussian process μ. We refer to a measure μ of the described form as a *hierarchical measure*.

To employ μ in a statistical or learning task, we have to sample from $M(\cdot|\boldsymbol{\theta})$ for a large number of parameter samples $\boldsymbol{\theta} \in \Theta$. In general, sampling requires a Cholesky factorization or spectral decomposition of $\mathbf{C}(\boldsymbol{\theta})$; see, e.g., [18, p. 1873]. We assume here that $\mathbf{C}(\boldsymbol{\theta})$ is a dense matrix. Then, sampling from $M(\cdot|\boldsymbol{\theta})$ in the standard way comes at a cost of $\mathcal{O}(n^3)$ operations for each $\boldsymbol{\theta} \in \Theta$. Since n is assumed to be very large, performing these tasks for many $\boldsymbol{\theta} \in \Theta$ becomes computationally infeasible.

For fixed $\boldsymbol{\theta}$, applying *adaptive cross approximation (ACA)* to $\mathbf{C}(\boldsymbol{\theta})$ has proven effective in accelerating the computation of a (partial) Cholesky factorization [20, 21, 36]. This is closely related to the Nyström method [46] which also builds approximations of a covariance matrix using a subset of its columns. Other than ACA, techniques employed for the fast generation of random fields are based on, e.g., circulant embedding [1, 8, 18], H-matrices [12, 27, 32], fractional stochastic partial differential equations [28, 30], or fast computations of truncated Karhunen-Loève expansions [6, 35, 37].

The main contribution of this article is a new variant, *parameter-dependent ACA*, that aims at approximating $\mathbf{C}(\cdot)$ simultaneously across the whole parameter range. For this purpose, we replace $\mathbf{C}(\cdot)$ by some low-rank approximation $\widehat{\mathbf{C}}(\cdot)$ for which sampling can be done computationally fast, even if n is large. We define the corresponding *approximate outer layer Markov kernel*

$$\widehat{M}(\cdot|\boldsymbol{\theta}) := \mathrm{N}(\mathbf{m}(\boldsymbol{\theta}), \widehat{\mathbf{C}}(\boldsymbol{\theta})) \qquad (\boldsymbol{\theta} \in \Theta)$$

and shallow Gaussian process $\widehat{\mu} := \mu' \widehat{M}$. In our method, $\widehat{\mathbf{C}}(\cdot)$ is constructed by a greedy procedure that controls the errors in the *Wasserstein* distance W_2. To be more precise, we aim at an approximation that is accurate in terms of the errors

$$\mathrm{W}_2\left(\mu, \widehat{\mu}\right), \qquad \mathrm{W}_2\left(M(\cdot|\boldsymbol{\theta}), \widehat{M}(\cdot|\boldsymbol{\theta})\right) \quad (\boldsymbol{\theta} \in \Theta). \tag{1}$$

This is a significant improvement compared to the heuristic algorithm proposed by Latz et al. [29]. Approximation methods that aim at controlling the approximation error are sometimes called *certified*. Further contributions of this work are the following:

- We propose and discuss techniques to approximate parameterized covariance matrices by linearly separable expansions, as required by ACA and other low-rank techniques,
- We analyze the robustness with respect to loss of positive semi-definiteness of the new parameter-dependent ACA and we demonstrate that it has linear cost $\mathcal{O}(n)$,
- We show computational experiments in which the techniques are used to construct low-rank approximations of matrices generated from Matérn covariance kernels; see, e.g., [39, Subsection 2.10].

This work is organized as follows. In Section 2, we compute upper bounds for the Wasserstein distances in eq. (1). These will be used for error control in the parameter-dependent ACA that we propose in Section 3. In Section 4, we give examples for isotropic covariance kernels and discuss approximation strategies that lead to linearly separable covariance kernels. Finally, we verify our theoretical findings in numerical experiments in Section 5 and conclude the work in Section 6.

2. **Error analysis.** As discussed in Section 1, the approximations $\widehat{\mu}, \widehat{M}$ of μ, M are obtained by replacing the parameterized covariance matrices by low-rank approximations. In this section, we quantify the error that is introduced by such an approximation.

Various distances for measures have been proposed, such as the total variation distance, the Hellinger distance, the Prokhorov metric, the Kullback–Leibler divergence, and the Wasserstein distance; we refer to Gibbs and Su [16] for an overview. Let $\boldsymbol{\theta} \in \Theta$. If $\widehat{\mathbf{C}}(\boldsymbol{\theta})$ is a low-rank approximation of $\mathbf{C}(\boldsymbol{\theta})$, typically $\mathrm{img}(\mathbf{C}(\boldsymbol{\theta})^{1/2}) \neq \mathrm{img}(\widehat{\mathbf{C}}(\boldsymbol{\theta})^{1/2})$. In this case, $M(\cdot|\boldsymbol{\theta})$ and $\widehat{M}(\cdot|\boldsymbol{\theta})$ are singular measures, which makes the total variation distance and equivalent metrics unsuitable: for singular measures the total variation distance is always equal to 2. The Wasserstein distance W_p, however, is suitable, as it is closely related to weak convergence; see [44, Theorem 6.9].

Definition 2.1 (Wasserstein)**.** Let $\nu, \widehat{\nu}$ be two probability measures on $(\mathbb{R}^n, \mathcal{B}\mathbb{R}^n)$. We define $\mathrm{Coup}(\nu, \widehat{\nu})$ to be the *set of couplings* of $\nu, \widehat{\nu}$, i.e. the set of probability measures H on $(\mathbb{R}^{2n}, \mathcal{B}\mathbb{R}^{2n})$, such that $H(B \times \mathbb{R}^n) = \nu(B)$, $H(\mathbb{R}^n \times B) = \widehat{\nu}(B)$ $(B \in \mathcal{B}\mathbb{R}^n)$. Given $p \in [1, \infty)$, the *Wasserstein(–p) distance* between ν and $\widehat{\nu}$ is defined by

$$\mathrm{W}_p(\nu, \widehat{\nu}) := \left(\inf_{H' \in \mathrm{Coup}(\nu, \widehat{\nu})} \int_{\mathbb{R}^{2n}} \|X_1 - X_2\|_p^p H'(\mathrm{d}X_1, \mathrm{d}X_2) \right)^{1/p},$$

provided that this integral is well-defined.

The Wasserstein distance W_p is motivated by the idea of optimal transport. It is defined as the cost of an optimal transport between the two probability measures, measured in the p-norm. The distance is well-defined if the pth absolute moment of both measures is finite. This is for instance the case for measures with light tails, such as the Gaussian measures that we encounter throughout Section 2.1. For more details on the Wasserstein distance, we refer to the book by Villani [44].

Throughout the rest of this paper, we assume, without loss of generality that the parameterized Gaussian measures have mean zero, i.e., $\mathbf{m} \equiv 0$.

2.1. **The fixed-parameter case.** We commence with the analysis of the Wasserstein distance W_2 for two Gaussian measures

$$\kappa := \mathrm{N}(0, C) := \mathrm{N}(0, \mathbf{C}(\boldsymbol{\theta})) := M(\cdot|\boldsymbol{\theta}), \qquad \widehat{\kappa} := \mathrm{N}(0, \widehat{C}) := \mathrm{N}(0, \widehat{\mathbf{C}}(\boldsymbol{\theta})) := \widehat{M}(\cdot|\boldsymbol{\theta}),$$

for *fixed* $\boldsymbol{\theta} \in \Theta$. A well-known result from [15] states that

$$\mathrm{W}_2(\kappa, \widehat{\kappa})^2 = \mathrm{trace}(C + \widehat{C} - 2(C^{1/2}\widehat{C}C^{1/2})^{1/2}). \tag{2}$$

Throughout the remainder of this section, we assume that $C - \widehat{C}$ is SPSD. Note that this assumption can be written as $\widehat{C} \preceq C$, where $\preceq$ denotes the *Löwner order* on $\mathrm{SPSD}(n)$. If this assumption holds, we can bound the Wasserstein distance W_2 between the measures κ and $\widehat{\kappa}$ in terms of the trace of $C - \widehat{C}$.

Lemma 2.2. *Let $\kappa := \mathrm{N}(0, C)$ and $\widehat{\kappa} := \mathrm{N}(0, \widehat{C})$ be Gaussian measures on $\mathbb{R}^n$ and let $C - \widehat{C}$ be SPSD. Then, $\mathrm{W}_2(\kappa, \widehat{\kappa}) \leq \mathrm{trace}(C - \widehat{C})^{1/2}$.*

Proof. The set of couplings $\mathrm{Coup}(\kappa, \widehat{\kappa})$ contains the following set of Gaussian measures on $\mathbb{R}^{2n}$:

$$E := \left\{ \mathrm{N}(0, G) : G = \begin{pmatrix} C & \Sigma \\ \Sigma^T & \widehat{C} \end{pmatrix}, \Sigma \in \mathbb{R}^{n \times n}, G \in \mathrm{SPSD}(2n) \right\} \subseteq \mathrm{Coup}(\kappa, \widehat{\kappa}).$$

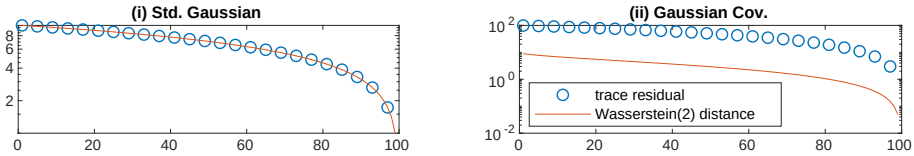


FIGURE 2. Wasserstein distance $\mathrm{W}_2(\kappa, \widehat{\kappa}_i)$ and trace residual $\mathrm{trace}(C - \widehat{C}^i)^{1/2}$ vs. i for the Gaussian measures considered in Example 2.3 (i)-(ii).

Let $H' \in E$. Then, by definition of W_2,

$$\begin{aligned}
\mathrm{W}_2(\kappa, \widehat{\kappa})^2 &\leq \int \|X_1 - X_2\|_2^2 H'(\mathrm{d}X_1, \mathrm{d}X_2) \\
&= \int \sum_{i=1}^{n} \left(X_1^{(i)} - X_2^{(i)}\right)^2 H'(\mathrm{d}X_1, \mathrm{d}X_2) \\
&= \int \sum_{i=1}^{n} \left(X_1^{(i)}\right)^2 + \left(X_2^{(i)}\right)^2 - 2\left(X_1^{(i)} X_2^{(i)}\right) H'(\mathrm{d}X_1, \mathrm{d}X_2) \\
&= \sum_{i=1}^{n} C_{ii} + \widehat{C}_{ii} - 2\Sigma_{ii} = \mathrm{trace}(C + \widehat{C} - 2\Sigma),
\end{aligned}$$

where $X_j = (X_j^{(1)}, \ldots, X_j^{(n)})$, $j = 1, 2$. The result of the lemma now follows from choosing $\Sigma = \widehat{C}$, provided that this choice leads to a measure in E, that is, the matrix

$$G = \begin{pmatrix} C & \widehat{C} \\ \widehat{C} & \widehat{C} \end{pmatrix}$$

is SPSD. On the other hand, this follows immediately from the fact that G can be written as a sum of two SPSD matrices:

$$G(\widehat{C}) = \begin{pmatrix} \widehat{C}^{1/2} \\ \widehat{C}^{1/2} \end{pmatrix} \begin{pmatrix} \widehat{C}^{1/2} \\ \widehat{C}^{1/2} \end{pmatrix}^T + \begin{pmatrix} C - \widehat{C} & 0 \\ 0 & 0 \end{pmatrix},$$

where $C - \widehat{C}$ is SPSD by assumption. □

Using the exact formula (2) for the Wasserstein distance, the following example verifies the tightness of the bound in Lemma 2.2.

Example 2.3. *Let $n = 100$. In two settings, we consider a measure $\kappa := \mathrm{N}(0, C)$ and a sequence of measures $\widehat{\kappa}_i = \mathrm{N}(0, \widehat{C}^i)$, $i = 1, ..., 100$.*

(i) We consider $C := \mathsf{Id}_{100}$ to be the identity matrix in $\mathbb{R}^{100\times 100}$ and $\widehat{C}^i$ to be the diagonal matrix with $\widehat{C}^i_{jj} = 1$, if $j \leq i$, and $\widehat{C}^i_{jj} = 0$, otherwise.

(ii) We consider $C := \left(\exp(-(j-k)^2)\right)_{1\leq j,k\leq 100}$ a discretization of the 1D Gaussian covariance kernel and $\widehat{C}^i := (i/100) \cdot C$.

Figure 2 shows $\mathrm{W}_2(\kappa, \widehat{\kappa}_i)$ and its upper bound in Lemma 2.2.

We observe that for Example 2.3(i), the bound from Lemma 2.2 coincides with the Wasserstein distance. This is not a coincidence, since one can show the following corollary.

Corollary 2.4. *Let* $\kappa := \mathrm{N}(0, C)$ *and* $\widehat{\kappa} := \mathrm{N}(0, \widehat{C})$*, where* $C - \widehat{C}$ *is SPSD. Additionally, suppose that* $C, \widehat{C}$ *commute and* $C^{1/2}\widehat{C}^{1/2} = \widehat{C}$*. Then,* $\mathrm{W}_2(\kappa, \widehat{\kappa}) = \mathrm{trace}(C - \widehat{C})^{1/2}$.

Proof. Since, C and $\widehat{C}$ commute, their square-roots commute as well, and hence it follows from (2) that

$$\begin{aligned}\mathrm{trace}(C + \widehat{C} - 2(C^{1/2}\widehat{C}C^{1/2})^{1/2}) &= \mathrm{trace}(C + \widehat{C} - 2(C^{1/2}\widehat{C}^{1/2}C^{1/2}\widehat{C}^{1/2})^{1/2}) \\ &= \mathrm{trace}(C - \widehat{C}),\end{aligned}$$

using $C^{1/2}\widehat{C}^{1/2} = \widehat{C}$. Taking the square-root on both sides proves our claim. □

Remark 2.5. The assumptions of Corollary 2.4 are for instance satisfied if $\widehat{C}$ is given via a truncation of the spectral decomposition of C. Such a low-rank approximation is given when employing a principal component analysis (PCA) or Karhunen-Loève (KL) expansion of the Gaussian random vectors with covariance C. In particular, let $V\mathrm{diag}(e_1, ..., e_n)V^{-1} = C$ be the spectral decomposition of C and $\widehat{C} := V\mathrm{diag}(\widehat{e}_1, ..., \widehat{e}_n)V^{-1}$, where some of the eigenvalues of C are replaced by zeros, i.e. $\widehat{e}_i \in \{e_i, 0\}$, $i = 1, ..., n$. The Wasserstein distance between mean-zero Gaussian measures with these two covariance matrices is then given by

$$W_2\left(\mathrm{N}(0, C), \mathrm{N}(0, \widehat{C})\right) := \left(\sum_{i=1}^{n} \mathbf{1}[\widehat{e}_i = 0]e_i\right)^{1/2}.$$

Notably, this is identical to the L^2 error obtained from dropping terms in the PCA.

For general low-rank approximations $\widehat{C}$ of C, we cannot expect the assumptions of Corollary 2.4 to hold. Clearly, in Example 2.3 (ii), the bound is not exact. However, it shows the same qualitative convergence behavior.

2.2. **The random-parameter case.** We now aim to generalize Lemma 2.2 to the hierarchical measures $\mu := \mu'\mathrm{N}(0, \mathbf{C})$ and $\widehat{\mu} := \mu'\mathrm{N}(0, \widehat{\mathbf{C}})$.

Theorem 2.6. *Let* μ' *be a probability measure on* Θ*,* $\mu := \mu'\mathrm{N}(0, \mathbf{C})$ *and* $\widehat{\mu} := \mu'\mathrm{N}(0, \widehat{\mathbf{C}})$*, where* $\mathbf{C}(\boldsymbol{\theta}) - \widehat{\mathbf{C}}(\boldsymbol{\theta})$ *is SPSD for* μ'*-a.e.* $\boldsymbol{\theta} \in \Theta$*. Moreover, we assume that* $\int \|X\|_2^2 \mu(\mathrm{d}X) < \infty$*. Then,*

$$\mathrm{W}_2(\mu, \widehat{\mu}) \leq \left(\int_\Theta \mathrm{trace}(\mathbf{C}(\boldsymbol{\theta}) - \widehat{\mathbf{C}}(\boldsymbol{\theta}))\mu'(\mathrm{d}\boldsymbol{\theta})\right)^{1/2}. \tag{3}$$

Proof. We proceed similarly as in the proof of Lemma 2.2. First, we define E to be the set

$$\left\{\mu'\mathrm{N}\left(0, \mathbf{G}(\cdot)\right) : \mathbf{G}(\boldsymbol{\theta}) = \begin{pmatrix} \mathbf{C}(\boldsymbol{\theta}) & \boldsymbol{\Sigma}(\boldsymbol{\theta}) \\ \boldsymbol{\Sigma}(\boldsymbol{\theta})^T & \widehat{\mathbf{C}}(\boldsymbol{\theta}) \end{pmatrix} \in \mathrm{SPSD}(2n), \right.$$
$$\left. \boldsymbol{\Sigma}(\boldsymbol{\theta}) \in \mathbb{R}^{n\times n} \ (\boldsymbol{\theta} \in \Theta, \mu'\text{-a.s.})\right\}.$$

One can show that $E \subseteq \mathrm{Coup}(\mu, \widehat{\mu})$. Let $H' \in E$. Then,

$$\begin{aligned}\mathrm{W}_2(\mu, \widehat{\mu})^2 &\leq \int \|X_1 - X_2\|_2^2 H'(\mathrm{d}X_1, \mathrm{d}X_2) = \int \sum_{i=1}^{n} \left(X_1^{(i)} - X_2^{(i)}\right)^2 H'(\mathrm{d}X_1, \mathrm{d}X_2) \\ &= \int \sum_{i=1}^{n} \left(X_1^{(i)}\right)^2 + \left(X_2^{(i)}\right)^2 - 2\left(X_1^{(i)}X_2^{(i)}\right) H'(\mathrm{d}X_1, \mathrm{d}X_2). \end{aligned} \tag{4}$$

By assumption, $\int \|X\|_2^2 \mu(\mathrm{d}X) < \infty$. Therefore,

$$\int \left(X^{(i)}\right)^2 \mu(\mathrm{d}X) < \infty, \quad \int \left(X^{(i)}\right)^2 \widehat{\mu}(\mathrm{d}X) < \infty,$$
$$\left| \int \left(X_1^{(i)} X_2^{(i)}\right) H'(\mathrm{d}X_1, \mathrm{d}X_2) \right| < \infty,$$

where the second moment of $\widehat{\mu}$ is finite, since $\mathbf{C}(\boldsymbol{\theta}) - \widehat{\mathbf{C}}(\boldsymbol{\theta})$ is almost surely SPSD. Hence, the integral in eq. (4) is finite, and

$$\begin{aligned}(4) &= \iint \sum_{i=1}^{n} \left(X_1^{(i)}\right)^2 + \left(X_2^{(i)}\right)^2 - 2\left(X_1^{(i)} X_2^{(i)}\right) \mathrm{N}(0, \mathbf{G}(\boldsymbol{\theta}))(\mathrm{d}X_1, \mathrm{d}X_2)\mu'(\mathrm{d}\boldsymbol{\theta}) \\ &= \int \sum_{i=1}^{n} \mathbf{C}(\boldsymbol{\theta})_{ii} + \widehat{\mathbf{C}}(\boldsymbol{\theta})_{ii} - 2\boldsymbol{\Sigma}(\boldsymbol{\theta})_{ii}\mu'(\mathrm{d}\boldsymbol{\theta}) \\ &= \int \mathrm{trace}(\mathbf{C}(\boldsymbol{\theta}) + \widehat{\mathbf{C}}(\boldsymbol{\theta}) - 2\boldsymbol{\Sigma}(\boldsymbol{\theta}))\mu'(\mathrm{d}\boldsymbol{\theta}),\end{aligned}$$

where $\boldsymbol{\Sigma}(\boldsymbol{\theta})$ is chosen such that $\mathbf{G}(\boldsymbol{\theta})$ is SPSD, $\boldsymbol{\theta} \in \Theta$, μ'-a.s. Analogously to the proof of Lemma 2.2, by setting $\boldsymbol{\Sigma}(\boldsymbol{\theta}) \equiv \widehat{\mathbf{C}}(\boldsymbol{\theta})$ we have that μ'-a.s. $\mathbf{G}(\boldsymbol{\theta})$ is SPSD. This yields the upper bound claimed in the theorem. □

In practice, we cannot compute the integral on the right-hand side of eq. (3). A straight-forward alternative is a Monte Carlo approximation with samples from μ'. We derive a Monte-Carlo-based bound in the corollary below and quantify its reliability.

Corollary 2.7. *Let $\boldsymbol{\theta}_1, ..., \boldsymbol{\theta}_M \sim \mu'$ be independent and identically distributed (i.i.d.) and* $\mathrm{Var}\left(\mathrm{trace}(\mathbf{C}(\boldsymbol{\theta}_1) - \widehat{\mathbf{C}}(\boldsymbol{\theta}_1))\right) < \infty$. *Then, for all $\varepsilon > 0$, we have*

$$\mathrm{W}_2(\mu, \widehat{\mu})^2 \leq \frac{1}{M} \sum_{m=1}^{M} \mathrm{trace}(\mathbf{C}(\boldsymbol{\theta}_m) - \widehat{\mathbf{C}}(\boldsymbol{\theta}_m)) + \varepsilon$$

with probability not less than $1 - \mathrm{Var}(\mathrm{trace}(\mathbf{C}(\boldsymbol{\theta}_1) - \widehat{\mathbf{C}}(\boldsymbol{\theta}_1)))/(M\varepsilon^2)$.

Proof. Let $\boldsymbol{\theta}_1, ..., \boldsymbol{\theta}_M$ be random variables defined on $(\Omega, \mathcal{F}, \mathbb{P})$ taking values in $(\Theta, \mathcal{A})$ and be distributed as stated above. Moreover, we define $\boldsymbol{\xi}_m := \mathrm{trace}(\mathbf{C}(\boldsymbol{\theta}_m) - \widehat{\mathbf{C}}(\boldsymbol{\theta}_m))$. for $m = 1, \ldots, M$.

By Theorem 2.6, we have $\mathrm{W}_2(\mu, \widehat{\mu})^2 \leq \mathbb{E}[\boldsymbol{\xi}_1]$. Hence,

$$\begin{aligned}\mathbb{P}\left(\mathrm{W}_2(\mu, \widehat{\mu})^2 \leq \frac{1}{M}\sum_{m=1}^{M} \boldsymbol{\xi}_m + \varepsilon\right) &\geq \mathbb{P}\left(\mathbb{E}[\boldsymbol{\xi}_1] \leq \frac{1}{M}\sum_{m=1}^{M} \boldsymbol{\xi}_m + \varepsilon\right) \\ &\overset{\varepsilon>0}{\geq} \mathbb{P}\left(|\mathbb{E}[\boldsymbol{\xi}_1] - \frac{1}{M}\sum_{m=1}^{M} \boldsymbol{\xi}_m| \leq \varepsilon\right) \\ &\geq 1 - \frac{\mathrm{Var}(\frac{1}{M}\sum_{m=1}^{M} \boldsymbol{\xi}_m)}{\varepsilon^2} \overset{\text{i.i.d.}}{=} 1 - \frac{\mathrm{Var}(\xi_1)}{M \cdot \varepsilon^2},\end{aligned}$$

where we employ the Chebyshev inequality in the second to last step. □

3. **Low-rank approximation of the covariance operator.**

3.1. **Cross approximation.** Cross approximation [3] is a technique to construct a low-rank approximation of a matrix from some of its rows and columns. More specifically, for a matrix $A \in \mathbb{R}^{n\times n}$ let us consider the rows $A(I,:)$ and columns $A(:,J)$ corresponding to index sets $I = \{i_1, \dots, i_k\}$ and $J = \{j_1, \dots, j_k\}$, respectively. Assuming that the cross matrix

$$A(I,J) = \begin{bmatrix} a_{i_1,j_1} & a_{i_1,j_2} & \cdots & a_{i_1,j_k} \\ a_{i_2,j_1} & a_{i_2,j_2} & \cdots & a_{i_2,j_k} \\ \vdots & \vdots & & \vdots \\ a_{i_k,j_1} & a_{i_k,j_2} & \cdots & a_{i_k,j_k} \end{bmatrix} \in \mathbb{R}^{k\times k}$$

is invertible, the cross approximation of A associated with I and J is given by

$$A(:,J)A(I,J)^{-1}A(I,:). \tag{5}$$

This approximation has rank $k = |I| = |J|$.

3.2. **Adaptive cross approximation for an SPSD matrix.** The choices of k and of the index sets I, J are crucial for the accuracy of the cross approximation (5). The *adaptive cross approximation* algorithm (ACA) chooses I, J in an adaptive way via a greedy strategy, analogous to complete pivoting in Gaussian elimination. In the first step of the procedure, i_1, j_1 are chosen such that the pivot element A_{i_1,j_1} has maximal absolute value. Then the procedure is repeated for A replaced by the residual matrix $A - A(:,i_1)A(i_1,j_1)^{-1}A(:,j_1)^T$, and so on. For an SPSD matrix A, the entry of maximal absolute value can always be found on the diagonal. As the residual matrix is again SPSD, this implies that ACA for SPSD matrices chooses index sets I, J such that $I = J$. This greatly reduces the cost of ACA because only the diagonal elements of the residual matrices need to be inspected in order to determine the pivot elements. Therefore, ACA has linear complexity with respect to n and returns an SPSD cross approximation of the form

$$A_I := A(:,I)A(I,I)^{-1}A(:,I)^T.$$

As the residual matrix $E_I := A - A_I$ is also SPSD, its trace equals its nuclear norm:

$$\|E_I\|_* := \sum_{j=1}^{n} \sigma_j(E_I) = \operatorname{trace}(E_I) = \operatorname{trace}(A - A(:,I)A(I,I)^{-1}A(:,I)^T), \tag{6}$$

with $\sigma_j(\cdot)$ denoting the jth singular value. In view of Lemma 2.2, if A is a covariance matrix then $\operatorname{trace}(E_I)^{1/2}$ is an upper bound for the squared Wasserstein distance W_2 between the Gaussian measures $\mathrm{N}(0,A)$ and $\mathrm{N}(0,A_I)$. The a priori error bound $\operatorname{trace}(E_I) \le 4^k(n-k)\sigma_{k+1}(A)$, where $k = |I|$, has been proved in [13, Theorem 1]. This estimate is pessimistic; typically ACA yields an approximation error that remains much closer to $\sigma_{k+1}(A)$.

The adaptive cross approximation algorithm for SPSD matrices [20] is reported in Algorithm 1. To simplify the description, E_I is initialized to the complete matrix A. In a practical implementation, only the diagonal elements of A are used and line 7 is replaced by updating the diagonal entries of E_I only. In turn, only the diagonal entries and the columns corresponding to I of A need to be evaluated. The cost of k iterations of Algorithm 1 is $\mathcal{O}((k + c_A)kn)$, where c_A denotes the cost of evaluating an entry of A.

Algorithm 1 Adaptive cross approximation for an SPSD matrix

procedure ACA($A, \mathsf{tol}, k_{\max}$)
  Set $E_I := A$, $k := 0$, $I := \emptyset$
  for $k := 1, 2, \ldots, k_{\max}$ **do**
    $i_k := \arg\max_i (E_I)_{ii}$
    $I \leftarrow I \cup \{i_k\}$
    $u_k := E_I(:, i_k)/\sqrt{(E_I)_{i_k i_k}}$
    $E_I := E_I - u_k u_k^T$
    if $\mathrm{trace}(E_I) \leq \mathsf{tol}$ **then**
      break
    end if
  end for
  return I
end procedure

3.3. **Adaptive cross approximation for a parameter-dependent SPSD matrix.** The approximation of a parameterized Gaussian random field requires the approximation of a parameterized family of covariance matrices, see Theorem 2.6. In this section we introduce an extension of ACA to the case of a parameterized family of matrices $A(\boldsymbol{\theta}) : \Theta \to \mathbb{R}^{n\times n}$ such that $A(\boldsymbol{\theta})$ has an affine linear expansion:

$$A(\boldsymbol{\theta}) = \varphi_1(\boldsymbol{\theta})A_1 + \cdots + \varphi_s(\boldsymbol{\theta})A_s, \quad \varphi_j : \Theta \to \mathbb{R}, \quad A_j \in \mathbb{R}^{n\times n}, \qquad j = 1, \ldots, s \tag{7}$$

and $A(\boldsymbol{\theta})$ is SPSD for each $\boldsymbol{\theta} \in \Theta$. Again, we aim at designing a matrix free method, so we assume to have an efficient way to extract entries from the matrices $A_1, \ldots, A_s$ in place of forming them explicitly. Moreover, we replace the parameter space Θ with a finite surrogate set $\Theta_f = \{\boldsymbol{\theta}_1, \ldots, \boldsymbol{\theta}_m\} \subset \Theta$, e.g. a uniform sampling over Θ or, in the light of Corollary 2.7, samples from μ'.

The goal of the algorithm is to provide a subset of indices I such that

$$A_I(\boldsymbol{\theta}) := A(\boldsymbol{\theta})(:, I)[A(\boldsymbol{\theta})(I, I)]^{-1} A(\boldsymbol{\theta})(:, I)^T \tag{8}$$

is a uniformly good approximation of $A(\boldsymbol{\theta})$, i.e. $\mathrm{trace}(A(\boldsymbol{\theta}) - A_I(\boldsymbol{\theta})) \leq \mathsf{tol}$ for any $\boldsymbol{\theta} \in \Theta_f$. Following a popular technique in reduced basis methods [23], the core idea of the method is to augment the set I with a greedy strategy. First, the value $\boldsymbol{\theta}^*$ which verifies

$$\mathrm{trace}(A(\boldsymbol{\theta}^*) - A_I(\boldsymbol{\theta}^*)) = \max_{\boldsymbol{\theta}\in\Theta_f} \mathrm{trace}(A(\boldsymbol{\theta}) - A_I(\boldsymbol{\theta})), \tag{9}$$

is identified. Then, one step of Algorithm 1 is applied to the matrix $A(\boldsymbol{\theta}^*) - A_I(\boldsymbol{\theta}^*)$ returning the new index that is appended to I.

The most expensive part of the method sketched above is finding $\boldsymbol{\theta}^*$ since it requires to evaluate the objective function for any point in Θ_f. In order to amortize the cost of multiple evaluations of $\mathrm{trace}(A(\boldsymbol{\theta}) - A_I(\boldsymbol{\theta})) = \mathrm{trace}(A(\boldsymbol{\theta})) - \mathrm{trace}(A_I(\boldsymbol{\theta}))$ we precompute once and for all

$$t_j := \mathrm{trace}(A_j), \quad j = 1, \ldots, s$$

so that for every $\boldsymbol{\theta} \in \Theta_f$, computing the quantity

$$\mathrm{trace}(A(\boldsymbol{\theta})) = \varphi_1(\boldsymbol{\theta})t_1 + \cdots + \varphi_s(\boldsymbol{\theta})t_s$$

requires $2s - 1$ flops and s evaluations of the scalar functions φ_j.

In addition, whenever I is updated, we store the matrices $A_1(I,I),\dots,A_s(I,I)$ and we compute the compact QR factorization $Q_I \in \mathbb{R}^{n\times sk}$, $R_I \in \mathbb{R}^{sk\times sk}$ of $[A_1(:,I),\dots,A_s(:,I)]$. In particular, for all $\boldsymbol{\theta}\in\Theta$ we have that

$$A(\boldsymbol{\theta})(:,I) = Q_I R_I \varphi(\boldsymbol{\theta}), \qquad \varphi(\boldsymbol{\theta}) := \begin{bmatrix} \varphi_1(\boldsymbol{\theta})\mathsf{Id}_k \\ \vdots \\ \varphi_s(\boldsymbol{\theta})\mathsf{Id}_k \end{bmatrix}.$$

By denoting with $R_A(\boldsymbol{\theta})$ the Cholesky factor of $A(\boldsymbol{\theta})(I,I)$, we can rewrite $\operatorname{trace}(A_I(\boldsymbol{\theta}))$ as follows:

$$\begin{aligned} \operatorname{trace}(A_I(\boldsymbol{\theta})) &= \operatorname{trace}(A(\boldsymbol{\theta})(:,I)[A(\boldsymbol{\theta})(I,I)]^{-1}A(\boldsymbol{\theta})(:,I)^T) \\ &= \operatorname{trace}(Q_I R_I \varphi(\boldsymbol{\theta}) R_A(\boldsymbol{\theta})^{-1} R_A(\boldsymbol{\theta})^{-T} \varphi(\boldsymbol{\theta})^T R_I^T Q_I^T) \\ &= \operatorname{trace}(R_A(\boldsymbol{\theta})^{-T}\varphi(\boldsymbol{\theta})^T R_I^T R_I \varphi(\boldsymbol{\theta}) R_A(\boldsymbol{\theta})^{-1}) \qquad (10) \\ &= \|R_I\varphi(\boldsymbol{\theta})R_A(\boldsymbol{\theta})^{-1}\|_F^2, \end{aligned}$$

where we used the cyclic property of the trace for deriving the third equality.

The considerations above lead to Algorithm 2.

Remark 3.1. *Instead of using the QR decomposition, the computation of* $\operatorname{trace}(A_I(\boldsymbol{\theta}))$ *can also be carried out by precomputing the quantities*

$$B_{ij} := A_i(:,I)^T A_j(:,I), \qquad i,j = 1,\dots,s$$

and exploiting the relation

$$\begin{aligned} \operatorname{trace}(A_I(\boldsymbol{\theta})) &= \operatorname{trace}(R_A(\boldsymbol{\theta})^{-T}A(\boldsymbol{\theta})(:,I)^T A(\boldsymbol{\theta})(:,I)R_A(\boldsymbol{\theta})^{-1}) \\ &= \operatorname{trace}(R_A(\boldsymbol{\theta})^{-T}B(\boldsymbol{\theta})R_A(\boldsymbol{\theta})^{-1}), \end{aligned}$$

where $B(\boldsymbol{\theta}) := \sum_{i,j=1}^s \varphi_i(\boldsymbol{\theta})\varphi_j(\boldsymbol{\theta})B_{ij}$. *This formula might be implemented in place of* (10) *which requires to compute the QR decomposition of* $A(\boldsymbol{\theta})(:,I)$. *However, forming the matrix* $B(\boldsymbol{\theta})$, *which is the principal submatrix of* $A(\boldsymbol{\theta})^2$ *corresponding to the index set* I, *causes a loss of accuracy in the evaluation of the stopping criterion. Due to the squaring of the singular values of* $A(\boldsymbol{\theta})(:,I)$, *the computed quantity is unreliable when* $\operatorname{trace}(E_I)$ *is below the square root of the machine precision.*

Note that the matrix Q_I in line 8 is actually not needed. More importantly, a careful implementation of Algorithm 2 recognizes that each $A_j(:,I)$ grows by a column at a time. Using QR updating techniques [17], the cost of executing line 8 in each outer loop is $\mathcal{O}(ns^2k)$ — instead of $\mathcal{O}(ns^2k^2)$ when computing the QR decomposition from scratch in each loop. Similarly, updating techniques could be used to accelerate the inner loop, but these are likely less important as long as s and k are much smaller than n. Without such techniques, one inner loop costs $\mathcal{O}(sk^3+s^2k^2)$. In summary, the total cost of executing k iterations of Algorithm 2 is $\mathcal{O}(ns^2k^2 + m(sk^4+s^2k^3))$. Additionally, $\mathcal{O}(kns)$ evaluations of entries from the coefficients A_j are needed.

3.4. **Robustness of ACA.** As we will explain in Section 4 the affine linear expansion (7) is often assured by an approximation of the true covariance operator. This approximation error may destroy positive semi-definitness, a property that is assumed throughout the derivations above. In this case, we propose to use the affine linear expansion only for identifying the index set I, i.e. as input of Algorithm 2, and then use the true covariance operator to form the cross approximation in the

Algorithm 2 Adaptive cross approximation for a parameterized family of SPSD matrices

procedure PARAM_ACA($A_1, \dots, A_s, \varphi_1, \dots, \varphi_s, \Theta_f, \mathsf{tol}$)
  Set $I := \emptyset$
  for $j := 1, \dots, s$ **do**
    $t_j := \mathrm{trace}(A_j)$
  end for
  for $k := 1, 2, \dots$ **do**
    Store matrices $A_1(I, I), \dots, A_s(I, I)$
    Compute R_I such that $Q_I R_I = [A_1(:, I), \dots, A_s(:, I)]$
    Set $\mathsf{res}_{\max} := 0$
    for $\boldsymbol{\theta} := \boldsymbol{\theta}_1, \dots, \boldsymbol{\theta}_m$ **do**
      Compute $A(\boldsymbol{\theta})(I, I) = \sum_{j=1}^{s} \varphi_j(\boldsymbol{\theta}) A_j(I, I)$
      Compute $R_A(\boldsymbol{\theta})$ such that $R_A(\boldsymbol{\theta})^T R_A(\boldsymbol{\theta}) = A(\boldsymbol{\theta})(I, I)$
      $\mathsf{res} = \sum_{j=1}^{s} \varphi_j(\boldsymbol{\theta}) t_j - \|R_I \varphi(\boldsymbol{\theta}) R_A(\boldsymbol{\theta})^{-1}\|_F^2$
      if $\mathsf{res} \geq \mathsf{res}_{\max}$ **then**
        $\mathsf{res}_{\max} = \mathsf{res}$ and $\boldsymbol{\theta}^* = \boldsymbol{\theta}$
      end if
    end for
    if $\mathsf{res}_{\max} \leq \mathsf{tol}$ **then**
      break
    end if
    $i_{\mathsf{new}} = \mathrm{ACA}(A(\boldsymbol{\theta}^*) - A_I(\boldsymbol{\theta}^*), 0, 1)$
    $I \leftarrow I \cup \{i_{\mathsf{new}}\}$
  end for
  return I
end procedure

online phase. This last step is essential to ensure that the residual matrix is still SPSD and its trace represents a bound for the Wasserstein distance with respect to the true covariance operator.

We remark that running Algorithm 1 on a symmetric indefinite matrix A returns an SPSD cross approximation A_I, because the method always chooses positive pivots. However, the stopping criterion at line 8 of Algorithm 1 loses its justification because the relation (6) between the trace and the nuclear norm does not hold. On the other hand, if A is very close to an SPSD matrix $\widetilde{A}$, then it is likely that I is a good choice for the cross approximation of $\widetilde{A}$. The next lemma establishes a result in this direction. The argument used in proof is inspired by the stability analysis of the pivoted Cholesky factorization [26, Section 10.3.1].

Lemma 3.2. *Consider symmetric matrices $A, E \in \mathbb{R}^{n \times n}$ such that $\widetilde{A} = A - E$ is SPSD and $\|E\|_2 \leq \delta$ for some $\delta > 0$. Let I be the index set returned by Algorithm 1 applied to A with tolerance* tol. *If $\rho := \delta \|A(I, I)^{-1}\|_2 < 1$ then*

$$\mathrm{trace}(\widetilde{A} - \widetilde{A}_I) \leq \mathsf{tol} + (n - k)\delta \frac{(1 + \|W\|_2)^2}{1 - \rho}$$

where $\widetilde{A}_I := \widetilde{A}(:, I)\widetilde{A}(I, I)^{-1}\widetilde{A}(I, :)$, $W := A(I, I)^{-1}A(I, I^c)$ and $I^c := \{1, \dots, n\} \setminus I$.

Proof. Consider the Schur complements

$$S = A(I^c, I^c) - A(I^c, I)A(I, I)^{-1}A(I, I^c), \qquad \widetilde{S} = \widetilde{A}(I^c, I^c) - \widetilde{A}(I^c, I)\widetilde{A}(I, I)^{-1}\widetilde{A}(I, I^c).$$

Because $\rho < 1$, the Neumann series gives

$$\widetilde{A}(I,I)^{-1} = A(I,I)^{-1} + \sum_{j>0} (A(I,I)^{-1}E(I,I))^j A(I,I)^{-1}.$$

This yields

$$\begin{aligned}\widetilde{S} &= S + E(I,I) + W^T E(I,I) \sum_{j\geq 0} [A(I,I)^{-1}E(I,I)]^j W \\ &+ E(I^c,I) \sum_{j\geq 0} [A(I,I)^{-1}E(I,I)]^j W + W^T \sum_{j\geq 0} [A(I,I)^{-1}E(I,I)]^j E(I,I^c) \\ &+ E(I^c,I) \sum_{j\geq 0} [A(I,I)^{-1}E(I,I)]^j A(I,I)^{-1} E(I,I^c),\end{aligned}$$

see also [26, Lemma 10.10]. In turn, $\|S-\widetilde{S}\|_2 \leq \delta \left(1 + \frac{\|W\|_2^2+2\|W\|_2+\rho}{1-\rho}\right) = \delta \frac{(1+\|W\|_2)^2}{1-\rho}$. Because S and $\widetilde{S}$ are symmetric matrices, standard eigenvalue perturbation results [17, Thm 8.1.5] imply that

$$|\lambda_j - \widetilde{\lambda}_j| \leq \delta \frac{(1+\|W\|_2)^2}{1-\rho},$$

where λ_j and $\widetilde{\lambda}_j$, $j = 1, \ldots, n-k$, denote the ordered eigenvalues of S and $\widetilde{S}$, respectively. This bound implies

$$\|\widetilde{S}\|_* = \sum_{j=1}^{n-k} \widetilde{\lambda}_j \leq \operatorname{trace}(S) + \sum_{j=1}^{n-k} |\lambda_j - \widetilde{\lambda}_j| \leq \mathsf{tol} + (n-k)\delta \frac{(1+\|W\|_2)^2}{1-\rho},$$

where the last inequality uses the stopping criterion $\mathsf{tol} \geq \operatorname{trace}(A - A_I) = \operatorname{trace}(S)$ of Algorithm 1. □

The upper bound in Lemma 3.2 indicates that the impact of the inexactness δ on the robustness of the trace criterion (6) may be magnified by the quantity $\|W\|_2^2$. Typically, $\|W\|_2^2$ remains moderate but it is difficult to provide a rigourous meaningful bound. The quite pessimistic bound $\|W\|_F^2 \leq \frac{1}{3}(n-k)(4^k-1)$ applies to some particular cases, see [26, Lemma 10.13].

An analogous result can be stated for the parameter dependent case where $\widetilde{A}(\boldsymbol{\theta})$ represents the full covariance operator, $A(\boldsymbol{\theta})$ is its linear separable approximation, and $E(\boldsymbol{\theta}) = A(\boldsymbol{\theta}) - \widetilde{A}(\boldsymbol{\theta})$ represents the approximation error. Since this generalization of Lemma 3.2 is rather straightforward we refrain from reporting it.

3.5. **ACA sampling and its complexity.** Let us now consider a parameterized Gaussian measure M, as introduced in Section 1, with linearly separable covariance operator $\mathbf{C} : \Theta \to \mathrm{SPSD}(n)$. In the following, we explain how the ACA approximation of $\mathbf{C}$ enables us to sample fast from an approximation of $M(\cdot|\boldsymbol{\theta})$ for a large number of $\boldsymbol{\theta} \in \Theta$.

After applying PARAM_ACA (Algorithm 2) to $\mathbf{C}$, we obtain the approximate parameterized matrix $\mathbf{C}_I : \Theta \to \mathrm{SPSD}(n)$ defined in (8). The corresponding approximate Markov kernel $\widehat{M}$ is given by $\widehat{M}(\cdot|\boldsymbol{\theta}) := \mathrm{N}(0, \mathbf{C}_I(\boldsymbol{\theta}))$. After this *offline phase*, we proceed with the *online phase*, that is, the sampling from $\widehat{M}$. For a given parameter $\boldsymbol{\theta} \in \Theta$, we compute the Cholesky factor $L \in \mathbb{R}^{k\times k}$ of $\mathbf{C}(\boldsymbol{\theta})(I,I)$. For a sample $\xi \sim \mathrm{N}(0, \mathrm{Id}_k)$ we have

$$\mathbf{C}(\boldsymbol{\theta})(:,I)L^{-T}\xi \sim \widehat{M}(\cdot|\boldsymbol{\theta}) = \mathrm{N}(0, \mathbf{C}_I(\boldsymbol{\theta})) \tag{11}$$

because

$$\begin{aligned}\mathbf{C}(\boldsymbol{\theta})(:,I)L^{-T}(\mathbf{C}(\boldsymbol{\theta})(:,I)L^{-T})^T &= \mathbf{C}(\boldsymbol{\theta})(:,I)L^{-T}L^{-1}\mathbf{C}(\boldsymbol{\theta})(:,I)^T \\ &= \mathbf{C}(\boldsymbol{\theta})(:,I)\mathbf{C}(\boldsymbol{\theta})(I,I)^{-1}\mathbf{C}(\boldsymbol{\theta})(:,I)^T = \mathbf{C}_I(\boldsymbol{\theta}).\end{aligned}$$

We now discuss the computational cost of drawing a sample from $\widehat{M}(\cdot|\boldsymbol{\theta})$ via (11). First, we need to construct the matrices $\mathbf{C}(\boldsymbol{\theta})(:,I), \mathbf{C}(\boldsymbol{\theta})(I,I)$ which comes at a cost of $\mathcal{O}(nks)$ if the linear expansion of $\mathbf{C}$ has s terms. Then, we compute the Cholesky factor L of $\mathbf{C}(\boldsymbol{\theta})(I,I)$ with $\mathcal{O}(k^3)$ operations, sample $\xi \sim \mathrm{N}(0, \mathrm{Id}_k)$, and solve $L^T b = \xi$ at a cost of $\mathcal{O}(k^2)$. Finally, the sample is obtained by the matrix vector product $\mathbf{C}(\boldsymbol{\theta})(:,I)b$, which costs another $\mathcal{O}(nk)$. In summary, the computational cost of one sample in the online phase is given by $\mathcal{O}(kns + k^3)$. Hence, the cost of the complete procedure for drawing $u \in \mathbb{N}$ samples is given by

$$\mathcal{O}(\underbrace{k^2ns^2 + m(k^4s + k^3s^2)}_{\text{offline}} + \underbrace{knsu + k^3u}_{\text{online}}).$$

Hence, the cost is linear in the size of the matrix n, the number of test parameters m, and the number u of different samples. As our approach is most meaningful in situations where the rank k is much smaller than n and s is small, the terms k^2ns^2 and $knsu$ will typically dominate the offline and online phases, respectively. Let us assume that applying the non-parameterized ACA u times costs $\mathcal{O}((\widetilde{k}+s)\widetilde{k}nu)$, with $\widetilde{k} \leq k$. Then, sampling with PARAM_ACA can be expected to be cheaper as long as $\widetilde{k}^2 > ks$ and m is not too large.

When the affine expansion (7) is an approximation of the true covariance operator, we use the latter both in the online phase of the approach based on PARAM_ACA and when applying the non-parameterized ACA. This changes the complexity of the two approaches by replacing the parameter s with the cost of evaluating one entry of the true covariance operator.

Remark 3.3. Working directly with the true covariance operator inside PARAM_ACA, i.e., identifying $\max_{\boldsymbol{\theta}\in\boldsymbol{\Theta}_f} \mathrm{trace}(A(\boldsymbol{\theta}) - A_I(\boldsymbol{\theta}))$ by applying $|I|$ steps of ACA for each value of $\boldsymbol{\theta}$, yields an overall cost of $\mathcal{O}(nmk^3)$ for the offline phase. Although this is a much simpler approach, it provides a significantly higher cost when considering fine discretizations of Θ.

4. **Isotropic covariance kernels.** Let $D \subseteq \mathbb{R}^\ell$ be some domain and $\|\cdot\|_D$ be a norm on D. A covariance kernel is a function $c : D \times D \to \mathbb{R}$ that is continuous, symmetric, and positive semidefinite. In the following, we consider *isotropic* covariance kernels c, which take

$$c(\mathbf{x}, \mathbf{y}) = \tilde{c}(\|\mathbf{x} - \mathbf{y}\|_D) \qquad \forall \mathbf{x}, \mathbf{y} \in D$$

for some function $\tilde{c} : [0, \infty) \to \mathbb{R}$. Such a kernel is invariant with respect to isometries, e.g., translations and rotations in the case of the Euclidean norm. Given points $\mathbf{x}_1, \ldots, \mathbf{x}_n \in D$, the covariance matrix $C \in \mathbb{R}^{n\times n}$ associated with c is defined by

$$C_{ij} = c(\mathbf{x}_i, \mathbf{x}_j) \qquad (i, j = 1, \ldots, n). \tag{12}$$

Parameterized covariance kernels are functions $c : D \times D \times \Theta \to \mathbb{R}$ such that $c(\cdot, \cdot; \boldsymbol{\theta})$ is a covariance kernel for any $\boldsymbol{\theta} \in \Theta$. The associated parameterized covariance matrix $\mathbf{C} : \Theta \to \mathbb{R}^{n\times n}$ is defined analogously as in (12).

4.1. **Examples.** The following examples of parameterized covariance kernels will be considered throughout the rest of this work. We refer to the work by Stein [39] for further examples.

Gaussian covariance. Let $D \subseteq \mathbb{R}^\ell$, $\ell \in \mathbb{N}$ and $\theta \in \Theta := [\underline{\theta}, \overline{\theta}]$ for $\underline{\theta} > 0$. We consider a Gaussian covariance kernel on D with correlation length θ defined as

$$c(\mathbf{x}, \mathbf{y}; \theta) = \sigma^2 \exp\left(-\frac{\|\mathbf{x}-\mathbf{y}\|_2^2}{2\theta^2}\right) \qquad (\mathbf{x}, \mathbf{y} \in D). \tag{13}$$

for some $\sigma^2 \in (0, \infty)$. The correlation length determines the strength of correlation between two points depending on their distance.

Matérn covariance. We let $D \subseteq \mathbb{R}^\ell$, $\ell \in \mathbb{N}$ and $\boldsymbol{\theta} \in \Theta := [\underline{\theta}, \overline{\theta}] \times (0, \infty]$ for $\underline{\theta} > 0$. The Matérn covariance kernel on D with correlation length θ_1 and smoothness θ_2 is defined as

$$c(\mathbf{x}, \mathbf{y}; \boldsymbol{\theta}) = \sigma^2 \frac{2^{1-\theta_2}}{\Gamma(\theta_2)} \left(\frac{\sqrt{2\theta_2}\|\mathbf{x}-\mathbf{y}\|_2}{\theta_1}\right)^{\theta_2} K_{\theta_2}\left(\frac{\sqrt{2\theta_2}\|\mathbf{x}-\mathbf{y}\|_2}{\theta_1}\right) \qquad (\mathbf{x}, \mathbf{y} \in D), \tag{14}$$

where Γ is the gamma function and K_{θ_2} is the modified Bessel function of second kind with parameter θ_2.

The correlation length has the same interpretation as for Gaussian kernels. Moreover, a Gaussian kernel with correlation length θ_1 can be viewed as a special case of a Matérn kernel by taking the limit $\theta_2 \to \infty$. For finite values, the parameter θ_2 determines the smoothness of the random samples; see, e.g., [40, Proposition 3.2] for details.

We aim at applying Algorithm 2 to obtain low-rank approximations of the covariance matrix $\mathbf{C}(\boldsymbol{\theta})$ associated with any of the parameterized covariance kernels above. However, the linear separability assumption (7) is not satisfied because the kernels depend nonlinearly on $\boldsymbol{\theta}$. To address this issue, an approximate linearization of Matérn kernels using Taylor expansion has been proposed in [29]. For smaller correlation lengths, this method becomes inefficient and we therefore discuss more general and more effective methods for linearising isotropic covariance kernels in the following.

4.2. **Linearization of isotropic covariance kernels.** Finding an (approximate) expansion (7) for $\mathbf{C}(\theta)$ is directly related to finding an expansion that separates the spatial variables from the parameters in the covariance kernel. To see this, let us consider a parameterized isotropic covariance kernel $c(\mathbf{x}, \mathbf{y}; \boldsymbol{\theta}) = \tilde{c}(\|\mathbf{x}-\mathbf{y}\|_2, \boldsymbol{\theta})$ with $\tilde{c} : [\underline{d}, \overline{d}] \times \Theta \to \mathbb{R}$, $\underline{d} = \min_D \|\mathbf{x}-\mathbf{y}\|_2$, and $\overline{d} = \max_D \|\mathbf{x}-\mathbf{y}\|_2$. If

$$\tilde{c}(d, \boldsymbol{\theta}) \approx \tilde{c}_s(d, \boldsymbol{\theta}) := \sum_{j=1}^{s} \varphi_j(\boldsymbol{\theta}) a_j(d) \tag{15}$$

for functions $\varphi_j : \Theta \to \mathbb{R}$ and $a_j : [\underline{d}, \overline{d}] \to \mathbb{R}$ then

$$c(\mathbf{x}, \mathbf{y}; \boldsymbol{\theta}) \approx c_s(\mathbf{x}, \mathbf{y}; \boldsymbol{\theta}) := \sum_{j=1}^{s} \varphi_j(\boldsymbol{\theta}) a_j(\|\mathbf{x}-\mathbf{y}\|_2). \tag{16}$$

By defining A_j to be the matrix associated with $a_j(\|\mathbf{x}-\mathbf{y}\|_2)$, as in (12), it follows that the matrix $\mathbf{C}_s(\boldsymbol{\theta})$ is associated with $c_s(\mathbf{x}, \mathbf{y}; \boldsymbol{\theta})$. Note that, unless (16) is an exact expansion, the matrices $\mathbf{C}_s(\boldsymbol{\theta})$ — while still being symmetric — are not guaranteed to be positive semi-definite for every $\boldsymbol{\theta} \in \Theta$. Lemma 3.2 indicates that ACA remains robust despite the loss of semi-definiteness and, assuming that the

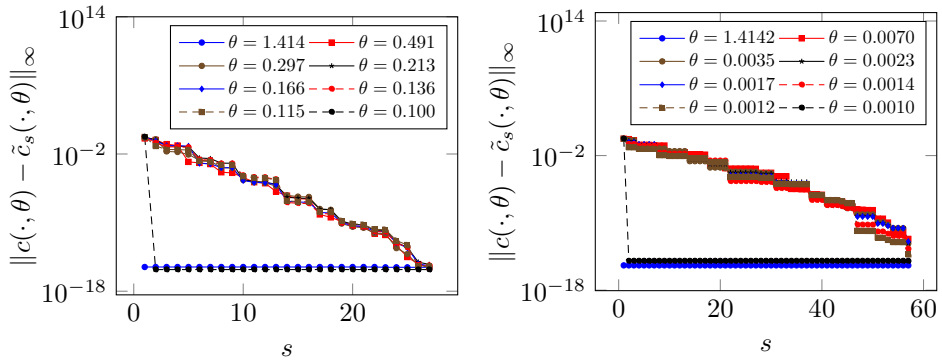


FIGURE 3. Gaussian covariance kernel. Error associated with the approximate covariance kernel $\tilde{c}_s$ vs. length of the expansion s, in the case $\theta \in [0.1, \sqrt{2}]$ (left) and $\theta \in [0.001, \sqrt{2}]$ (right). Each curve represents the infinity norm $\|c(\cdot,\theta) - \tilde{c}_s(\cdot,\theta)\|_\infty$ for a fixed value of θ, approximated by taking the maximum over 500 equispaced values for d in $[0, \sqrt{2}]$.

tolerance of ACA is on the level of the approximation error of (15) then the total error committed by ACA and the expansion can be expected to stay on the same level.

The separable expansion (15) is the continuous analogue of low-rank matrix approximation. Several methods have been proposed to address this task, see, e.g., [4, 41, 33]. In the following sections we describe how we compute such an expansion depending on the number of parameters.

4.2.1. *1D parameter space.* When there is only one parameter θ and Θ is an interval then $\tilde{c}(d,\theta)$ becomes a bivariate function on a rectangular domain. In this situation we can apply the continuous analogue of the ACA for bivariate functions [4]. To implement this method in practice, it needs to be combined with a discretization of the variables. In [42], the Chebyshev expansion is proposed for the latter, an approach implemented in the command `cdr` of the toolbox Chebfun2, which is used in our experiments.

Example 4.1. *Let us consider the Gaussian covariance kernel from Section 4.1 with* $D = [0,1]^2$, *so that* $[\underline{d}, \overline{d}] = [0, \sqrt{2}]$ *and* $\Theta = [0.1, \sqrt{2}]$. *The accuracy of the separable expansion* (16) *— computed via the Chebfun2 command* `cdr` *— is shown in Figure 3 (left); we plot the maximum absolute error* $\max_{d\in[0,\sqrt{2}]} |\tilde{c}(d,\theta) - \tilde{c}_K|$ *— as* K *increases — for different choices of* θ *in* Θ. *We remark that — already for* $K = 1, 2$ *—* $\tilde{c}_K$ *is accurate when considering* $\theta = \underline{\theta} = 0.1$ *and* $\theta = \overline{\theta} = \sqrt{2}$ *because the ACA for functions selects those values of* θ *as pivots.*

We repeat the experiment for a smaller minimal correlation length $\underline{\theta} = 0.001$. *This case is problematic when using polynomial expansions for performing the approximation* (15)*; see the results reported in* [29]. *Although its convergence is somewhat slower, the ACA for functions still performs reasonably well; see Figure 3 (right).*

4.2.2. *Multidimensional parameter space.* In the case of a multidimensional Θ we rely on a slight modification of the so called *empirical interpolation method* (EIM) [2]. Before sketching the procedure, we recall the notion of *quasimatrix* [43].

Definition 4.2. Let $C([\underline{d}, \overline{d}])$ be the set of continuous real functions on $[\underline{d}, \overline{d}]$ and $r \in \mathbb{N}$. An $[\underline{d}, \overline{d}] \times r$ quasimatrix is an ordered r-tuple of functions in $C([\underline{d}, \overline{d}])$.

The name quasimatrix comes from the representation of a generic tuple $(f_1(d), \dots, f_r(d))$ as a $[\underline{d}, \overline{d}] \times r$ matrix $F := [f_1(d)| \dots |f_r(d)]$ where the continuous row index refers to the argument d while the discrete column index selects the function. Common operations for matrices can be easily extended to quasimatrices. For instance, given a finite set $\mathcal{I} = \{d_1, \dots, d_s\} \subset [\underline{d}, \overline{d}]$ we define

$$F(\mathcal{I}, :) := \begin{bmatrix} f_1(d_1) & \dots & f_r(d_1) \\ \vdots & & \vdots \\ f_1(d_s) & \dots & f_r(d_s) \end{bmatrix} \in \mathbb{R}^{s \times r}.$$

Intuitively, the product $F \cdot M$ with $M \in \mathbb{R}^{r \times p}$ is defined as the $[\underline{d}, \overline{d}] \times p$ quasimatrix whose columns are linear combinations of the columns of F. Moreover, the most used matrix factorizations, e.g. LU, QR and SVD, can be extended to quasimatrices [43]. Analogously, we define r-tuple of real functions of $\boldsymbol{\theta}$ as transposed quasimatrices, i.e. $r \times \Theta$ matrices, and the corresponding matrix operations. The algorithm that we employ for computing the affine linear expansion (7) combines EIM with the SVD of quasimatrices. It proceeds as follows:

1. Generate samples $\boldsymbol{\theta}_1, \dots, \boldsymbol{\theta}_r$ from Θ.
2. Define the snapshot functions $\hat{c}_j(d) := \tilde{c}(d, \boldsymbol{\theta}_j)$, $j = 1, \dots, r$ and form the quasi-matrix
$$F = \left[\hat{c}_1(d)| \dots |\hat{c}_r(d)\right] \in \mathbb{R}^{[\underline{d}, \overline{d}] \times r}.$$
3. Compute the SVD of F:
$$F = U \Sigma V^*, \quad U \in \mathbb{R}^{[\underline{d}, \overline{d}] \times r}, \quad \Sigma, V \in \mathbb{R}^{r \times r}.$$
Truncate the SVD decomposition by keeping the first s columns of $u_1(d), \dots, u_s(d)$ of U, which corresponds to the diagonal entries in Σ that are above a prescribed tolerance τ.
4. Determine a set $\mathcal{I} = \{d_1, \dots, d_s\}$ of nodes for interpolation by using the greedy strategy of EIM, reported in Algorithm 3.
5. Set $a_j(\mathbf{x}, \mathbf{y}) := u_j(\|\mathbf{x} - \mathbf{y}\|_2)$, $j = 1, \dots s$ and define the functions $\varphi_j(\boldsymbol{\theta})$ via the transposed quasimatrix which solves the linear system
$$\begin{bmatrix} u_1(d_1) & \dots & u_s(d_1) \\ \vdots & \dots & \vdots \\ u_1(d_s) & \dots & u_s(d_s) \end{bmatrix} \begin{bmatrix} \varphi_1(\boldsymbol{\theta}) \\ \vdots \\ \varphi_s(\boldsymbol{\theta}) \end{bmatrix} = \begin{bmatrix} \tilde{c}(d_1, \boldsymbol{\theta}) \\ \vdots \\ \tilde{c}(d_s, \boldsymbol{\theta}) \end{bmatrix}.$$

The whole procedure is reported in Algorithm 4. The practical implementation makes again use of the toolbox Chebfun2 which provides all the functionalities for handling quasimatrices.

The sampling at step 1 can be performed via a greedy algorithm, as in [2], or with other strategies that aim at mitigating the curse of dimensionality when considering a high dimensional parameter space [5, 24, 31]. Since in our numerical tests we do not need to deal with very high dimensional parameter spaces, we just perform a

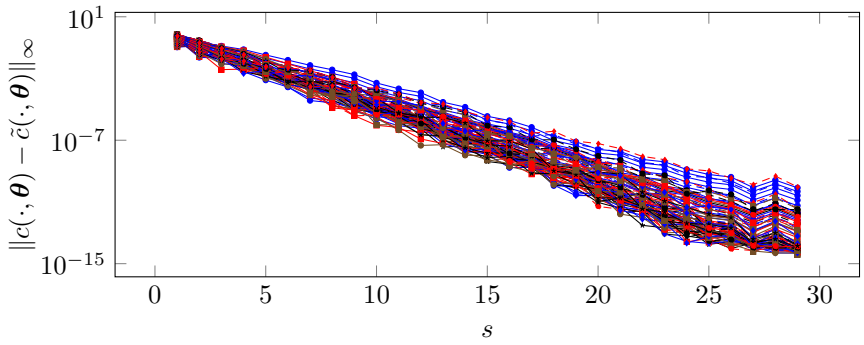


FIGURE 4. Matérn covariance kernel. Error associated with the approximate covariance kernel $\tilde{c}_s$ vs. length of the expansion s, for $(\theta_1, \theta_2) \in [0.1, \sqrt{2}] \times [2.5, 7.5]$. Each curve represents the infinity norm $\|c(\cdot, \boldsymbol{\theta}) - \tilde{c}_s(\cdot, \boldsymbol{\theta})\|_\infty$ for a fixed pair $\boldsymbol{\theta} = (\theta_1, \theta_2)$, approximated by taking the maximum over 500 equispaced values for d in $[0, \sqrt{2}]$.

tensorized equispaced sampling of Θ. The accuracy of Algorithm 4 is tested in the following example.

Example 4.3. *Let us consider the Matérn covariance kernel from Section 4.1 with* $diam(D) = \sqrt{2}$, $\theta_1 \in [0.1, \sqrt{2}]$ *and* $\theta_2 \in [2.5, 7.5]$. *The accuracy of the separable expansion* (16) *— computed via Algorithm 4 — is shown in Figure 4; each curve represents the maximum absolute error* $\max_{d \in [0,\sqrt{2}]} |\tilde{c}(d, \boldsymbol{\theta}) - \tilde{c}_s(d, \boldsymbol{\theta})|$ *— as* s *increases — for* $\boldsymbol{\theta} = (\theta_1, \theta_2)$ *chosen on a* 10×10 *grid obtained as tensor product of equispaced values on* $[0.1, \sqrt{2}]$ *and* $[2.5, 7.5]$, *respectively. The maximum of the error is approximated by taking its largest value over* 500 *equispaced samples of* d *in* $[0, \sqrt{2}]$.

Algorithm 3 Interpolation nodes selection

procedure node_selection($u_1(d), \ldots, u_K(d)$) ▷ real functions defined on $[\underline{d}, \overline{d}]$
1: Set $d_1 = \arg\max_{[\underline{d},\overline{d}]} |u_1(d)|$, $\mathcal{I} = \{d_1\}$, $U = [u_1(d)]$
2: **for** $j := 2, \ldots, s$ **do**
3: $c \leftarrow U(\mathcal{I}, 1 : j-1)^{-1} u_j(\mathcal{I})$
4: $r(d) \leftarrow u_j(d) - U \cdot c$
5: $d_j \leftarrow \arg\max_{[\underline{d},\overline{d}]} |r(d)|$
6: $U \leftarrow [U, u_j(d)]$, $\mathcal{I} \leftarrow \mathcal{I} \cup \{d_j\}$
7: **end for**
8: **return** $\mathcal{I}$

5. **Numerical experiments.** We test the performance of Algorithm 2 for the examples discussed in the previous section. All experiments have been carried out on a Laptop with a dual-core Intel Core i7-7500U 2.70 GHz CPU, 256KB of level 2 cache, and 16 GB of RAM. The algorithms are implemented in Matlab and tested under MATLAB2019a, with MKL BLAS version 2018.0.3 utilizing both cores.

Algorithm 4 Empirical Interpolation method

procedure EIM($\tilde{c}(d, \boldsymbol{\theta})$, τ) ▷ $\tilde{c}$ real function defined on $[\underline{d}, \overline{d}] \times \Theta$
Sample $\boldsymbol{\theta}_1, \dots, \boldsymbol{\theta}_r$ from Θ
Set $F = [\tilde{c}(d, \boldsymbol{\theta}_1) | \dots | \tilde{c}(d, \boldsymbol{\theta}_r)] \in \mathbb{R}^{[\underline{d}, \overline{d}] \times r}$
$[U, \Sigma, V] \leftarrow \mathrm{svd}(F)$
Compute s s.t. $\Sigma_{s,s} > \tau > \Sigma_{s+1,s+1}$
$\mathcal{I} \leftarrow$ node_selection$(U(:,1), \dots, U(:,s))$
$U_s \leftarrow U(\mathcal{I}, 1:s)$
for $j = 1, \dots s$ **do**
    $a_j(\boldsymbol{x}, \boldsymbol{y}) \leftarrow U(\|\boldsymbol{x} - \boldsymbol{y}\|_2, j)$
    $\varphi_j(\boldsymbol{\theta}) \leftarrow e_j^T U_s^{-1} \tilde{c}(\mathcal{I}, \boldsymbol{\theta})$ ▷ e_j j-th vector of the canonical basis
end for
return $a_1, \dots, a_s, \varphi_1, \dots, \varphi_s$

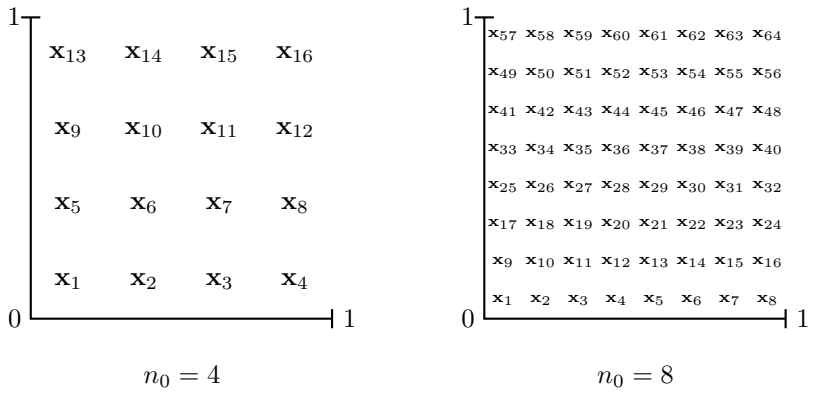


FIGURE 5. Schematic of the definitions of the nodes $\mathbf{x}_1, \dots, \mathbf{x}_n$, for $n_0 \in \{4, 8\}$.

5.1. **Parameterized Gaussian covariance kernel.** Let us consider a hierarchical Gaussian random field on $D = [0,1]^2$ with mean $\mathbf{0}$ and covariance operator induced by the Gaussian covariance kernel $c(\mathbf{x}, \mathbf{y}; \theta)$ defined in (13) with $\theta \in \Theta = [0.1, \sqrt{2}]$. The finite surrogate Θ_f of the parameter space is obtained by taking equispaced points on Θ. The approximate linearized kernel $\widetilde{c}_s$ is retrieved via the function-valued ACA as in Example 4.1. The cut-off value is set to $s = 18$ which provides, according to the results shown in Figure 3, a cut-off error of about 10^{-8}.

We discretize the random field on a regular grid with $n := n_0^2$ grid points. In turn, the matrix $\mathbf{C}(\theta) \in \mathbb{R}^{n \times n}$ is given by

$$\mathbf{C}(\theta)_{i,j} := \frac{1}{n} \cdot c\left(\mathbf{x}_i, \mathbf{x}_j; \theta\right) \qquad (i, j = 1, \dots, n),$$

$$\mathbf{x}_i := \left(\frac{\mathrm{mod}(i, n_0) + 0.5}{n_0 + 1}, \frac{\mathrm{div}(i, n_0) + 0.5}{n_0 + 1} \right)^T \qquad (i = 1, \dots, n),$$

where $\mathrm{div}(i, n_0)$ represents the integer division of i by n_0 and $\mathrm{mod}(i, n_0)$ represents the associated remainder term. We illustrate the node positions with associated

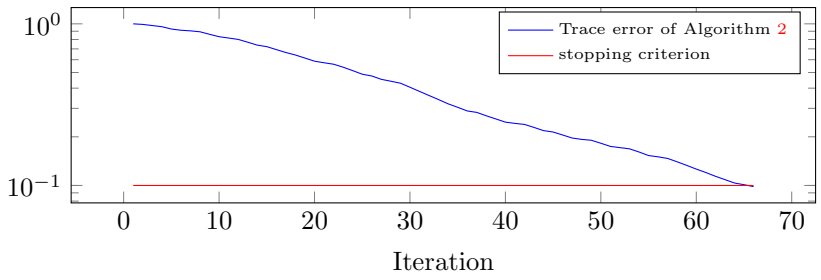


FIGURE 6. Test 1. Error vs. number of iterations for Algorithm 2 applied to a discretized Gaussian covariance operator.

indices in Figure 5. Note that this covariance matrix corresponds to a finite element discretization of the random field using piecewise constant ansatzfunctions with square supports and quadrature with one node in the centre of each of the supports.

Remark 5.1 (BTTB)**.** Note that the matrix $\mathbf{C}(\theta)$ is *Block Toeplitz with Toeplitz Blocks* (BTTB). This is caused by the regular distribution of the nodes and the isotropy of the covariance kernel. For covariance matrices with this structure, efficient low-rank approximation [19] and sampling strategies (circulant embedding) are available. Note that, our ACA method does neither require this structure nor profit from it. Thus, the results discussed in the following extend to covariance matrices that are not BTTB which arise — for instance — when considering more complex geometries D or irregular discretizations.

Test 1. As a first test, we set $n_0 = 512$, i.e. $n \approx 2.6 \cdot 10^5$ degrees of freedom and the cardinality of Θ_f to 1000. Then, we run Algorithm 2 using $\mathrm{tol} = 10^{-1}$ as value for the tolerance at line 8 of Algorithm 1. This tolerance guarantees that a KL expansion with the same Wasserstein(2) error would represent 90% of the random field's variance; this is a usual choice in random field discretizations (see Remark 2.5).

The evolution of the trace error as the algorithm proceeds is shown in Figure 6. The algorithm terminates after 65 iterations meaning that a 65-dimensional basis is sufficient to represent the parameter-dependent $512^2 \times 512^2$ operator with the desired accuracy. Note that Algorithm 2 always picks the smallest correlation length $\theta^* = 0.1$ in the for-loop beginning in line 10.

The computational time of the algorithm is 336.8 seconds. We remark that the updating strategy for the QR factorization at line 8 of Algorithm 2, described in Section 3.3, is crucial. Indeed, computing the QR factorization from scratch in each iteration increases the execution of Algorithm 2 to 1593.3 seconds; 80% of which are spent on line 8.

Test 2. In order to shed some light on the role played by θ, Figure 7 shows the sorted eigenvalues of $\mathbf{C}(\theta)$ for $\theta \in [0.1, \sqrt{2}]$ when using $n_0 = 128$ for the discretization. We conclude that a smaller correlation length leads to a slower eigenvalue decay. Consequently, a small value of θ implies that a larger rank in a low-rank approximation of $\mathbf{C}(\theta)$ is needed in order to retain the same accuracy.

Test 3. We have measured the execution time of Algorithm 2 for the example described above with $n_0 \in \{2^3, \dots, 2^9\}$ and $|\Theta_f| \in \{10, 10^2, 10^3, 10^4\}$. The timings shown in Figure 8 (left) are averaged over three runs. It can be seen that n influences the cost linearly, as predicted by the complexity estimates derived in Section 3.3.

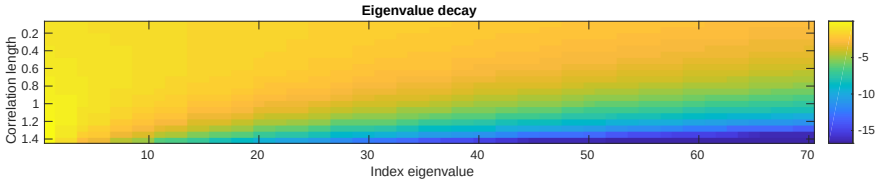
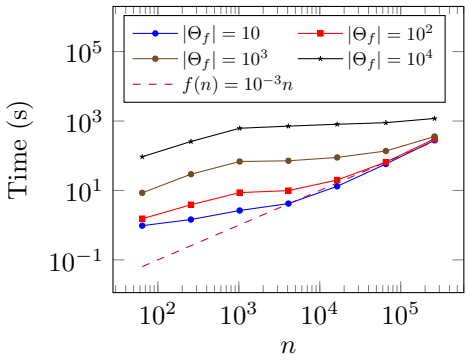


FIGURE 7. Test 2. Decimal logarithms of the largest 70 eigenvalues $\mathbf{C}(\theta)$ for different values of $\theta \in [0.1, \sqrt{2}]$ and $n_0 = 128$.



Ranks

10^4	47	58	61	62	64	65	65
10^3	47	58	61	62	64	65	65
10^2	47	58	61	62	64	65	65
10	47	58	61	62	64	65	65
	2^6	2^8	2^{10}	2^{12}	2^{14}	2^{16}	2^{18}

FIGURE 8. Test 3. Timings in seconds (left) and ranks (right) obtained from the ACA algorithm applied to different discretizations of the covariance operator. The x-axes of both figures show the degrees of freedom $n = n_0^2$ of the discretized covariance operators. The y-axes show the mean elapsed time over three runs for the figure on the left and the quantity $|\Theta_f|$ for the table on the right.

Moreover, we reported the rank of the ACA approximation, i.e. the cardinality of the index set I returned by Algorithm 2, in Figure 8 (right). We see that the rank converges to 65, when refining the random field, suggesting that the rank obtained with ACA might be discretization invariant. Also the rank seems to not be influenced at all by the cardinality of Θ_f since the algorithm always chooses the smallest correlation length. In this particular setting, the outcome of the algorithm does not change, as long as $\underline{\theta}$ does not vary.

Test 4. Now, we compare the convergence history of the method with the nuclear norm of the error and the trace error of the best low-rank approximations of $\mathbf{C}(\theta)$. We remark that the convergence history of Algorithm 2 corresponds to the trace error with respect to the approximate covariance kernel, i.e. the quantity $\max_{\theta\in\Theta_f} \operatorname{trace}(\mathbf{C}_s(\theta) - \mathbf{C}_{sI}(\theta))$. Since the approximate covariance kernel is not guaranteed to be SPSD, as true measure of the error we consider the maximum nuclear norm of $\mathbf{C}(\theta) - \mathbf{C}_{sI}(\theta)$ over $\theta \in \Theta_f$. Finally, since $\mathbf{C}_{sI}(\theta)$ is a rank $k = |I|$ matrix for each value of θ, we also compute the benchmark quantity $\max_{\theta\in\Theta_f} \operatorname{trace}(\mathbf{C}(\theta) - \mathbf{C}_{(k)}(\theta))$, where $\mathbf{C}_{(k)}(\theta)$ denotes the truncated SVD of length k of $\mathbf{C}(\theta)$.

We run Algorithm 2 on an example of small dimension: $n_0 = 20$ and $|\Theta_f| = 200$. Then, we plot the three quantities discussed above in Figure 9. We see that the trace error computed by Algorithm 2 and the nuclear norm of the error coincide

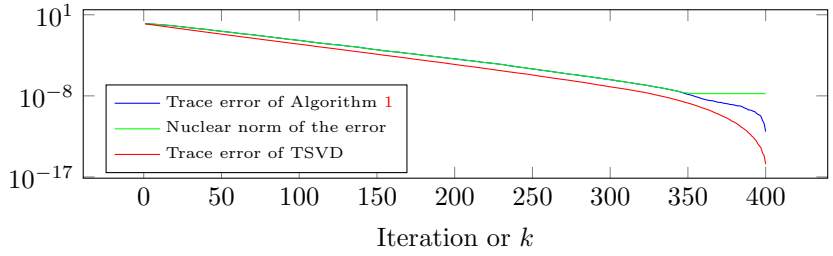


FIGURE 9. Test 4. Comparison between the convergence history of Algorithm 1 (blue), the maximum nuclear norm of $\mathbf{C}(\theta) - \mathbf{C}_{sI}(\theta)$ over Θ_f (green) and the best trace error associated with the truncated SVDs $\max_{\theta\in\Theta_f} \mathrm{trace}(\mathbf{C}(\theta) - \mathbf{C}_{(k)}(\theta))$ (red).

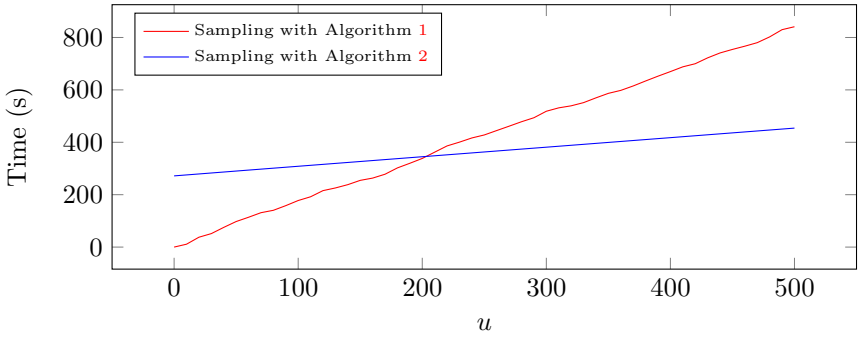


FIGURE 10. Test 5. Time consumption vs. number of samples for the sampling strategies based on Algorithm 1 and Algorithm 2, applied to a discretized Gaussian covariance operator.

as far as they stay above 10^{-8}. Then, the nuclear norm of the error stagnates because we have reached the level of inexactness which affects the approximate linear separable expansion. To conclude, we observe that the trace error associated with the truncated SVDs decays only slightly faster confirming the good convergence rate of the approximation returned by Algorithm 2.

Test 5. We conclude the experiments on the Gaussian kernel by testing the sampling strategy proposed in Section 3.5 for $n_0 = 512$, and $|\Theta_f| = 100$. More specifically, we consider the task of sampling u values of θ from a uniform distribution on $[0.1, \sqrt{2}]$ and — for each of those values — generating one sample from $\mathrm{N}(0, \mathbf{C}(\theta))$. Our strategy is to run Algorithm 2 to get the approximated kernel operator $\mathbf{C}_I(\cdot)$ and then sample from $\mathrm{N}(0, \mathbf{C}_I(\theta))$ as described in Section 3.5. We compare this method with applying Algorithm 1 directly on $\mathbf{C}(\theta)$ for each sample of θ. The timings of the two approaches, as the number of samples increases, are reported in Figure 10. Notice that, the time consumption of the strategy based on Algorithm 2 starts from a positive value which indicates the cost of the offline phase. We see that, while both methods have linear costs with repsect to u, the online phase of our strategy is faster by a factor about 4.6 than generating one sample with Algorithm 1. In our test, about 200 samples are enough to amortize the cost of the offline phase and to make our algorithm more convenient.

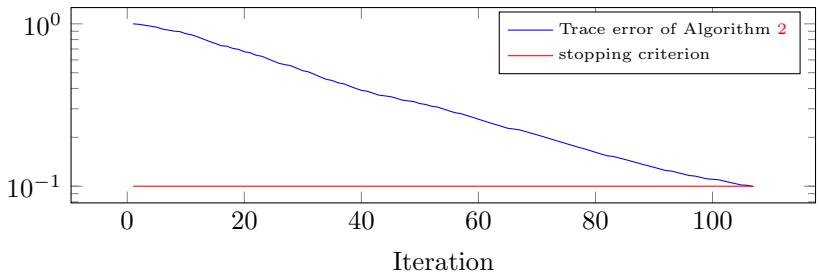


FIGURE 11. Error vs. number of iterations for Algorithm 2 applied to a discretized 2D Matérn kernel with $\theta_1 \in [0.1, \sqrt{2}]$ and $\theta_2 = 2.5$.

5.2. **Parameterized Matérn covariance kernel with slower eigenvalue decay.** In this section, we modify the parameterized random field considered in Section 5.1 by replacing the Gaussian covariance kernel with the Matérn covariance kernel defined in (14) with $\theta_1 \in [0.1, \sqrt{2}]$ and $\theta_2 = 2.5$. Also here, we make use of an approximate linearized kernel $\widetilde{c}_K$ — computed via the function-valued ACA — with cut-off value $s = 18$ which again provides an approximation error of about 10^{-8}. This ensures that the approximation error of $\tilde{c}_s$ does not affect the convergence history of Algorithm 2 in the considered example.

The samples with this covariance kernel are only twice continuously differentiable, as opposed to the analytic samples from the Gaussian covariance kernel. Hence, we expect a larger numerical rank of the associated covariance matrix $\mathbf{C}(\theta)$ and a larger rank when employing the ACA algorithm.

We run Algorithm 2 with $n = n_0^2 = 512^2$, $|\Theta_f| = 1000$ and $\mathrm{tol} = 10^{-1}$. The evolution over the iterations of the trace error computed by Algorithm 2 is reported in Figure 11. The algorithm terminates after 106 iterations, and it takes 1015.9 seconds, averaged over a total of three runs. It thus takes about 3 times longer than a similar experiment with the Gaussian kernel. As expected, the rank that we obtain is indeed larger than before. On the other hand, a 106-dimensional basis is still suitably small to efficiently represent a parameter dependent matrix of size $512^2 \times 512^2$.

6. **Conclusions.** We have proposed and analyzed a new method for the low-rank approximation of the Cholesky factor of a parameter dependent covariance operator. The approximation returned by our algorithm is certified, in the sense that it guarantees an upper bound for the error in the Wasserstein distance W_2 between mean-zero Gaussian measures having the true and low-rank covariance matrix, respectively. Algorithm 2 leads naturally to a fast sampling procedure for parameterized Gaussian random fields and potentially for the efficient treatment of certain Bayesian inverse problems [10, 29]. Beyond Gaussian random fields, the parameter-dependent ACA method can be applied in much more general hierarchical, kernel-based learning tasks. Consider, e.g., a non-linear support vector machine with parameterized (i.e. shallow), isotropic, symmetric, and positive semi-definite kernels that shall be trained with a large amount of data. Here, the ACA leads to a natural compression of the kernel matrix. Analysing the error introduced by ACA in other learning tasks would be an interesting topic for future work.

There is also other potential for future work. For example, while we have observed experimentally, for the examples tested, that Algorithm 2 returns an index set I of low cardinality that yields a good approximation $A_I(\boldsymbol{\theta})$ for all parameter values, it would be interesting to derive a prior existence results based on properties of the kernel.

REFERENCES

[1] M. Bachmayr, I. G. Graham, V. Kien Nguyen and R. Scheichl, Unified analysis of periodization-based sampling methods for Matérn covariances, *arXiv preprint arXiv:1905.13522*.

[2] M. Barrault, Y. Maday, N. C. Nguyen and A. T. Patera, An 'empirical interpolation' method: application to efficient reduced-basis discretization of partial differential equations, *C. R. Math. Acad. Sci. Paris*, **339** (2004), 667–672.

[3] M. Bebendorf, Approximation of boundary element matrices, *Numer. Math.*, **86** (2000), 565–589.

[4] M. Bebendorf, Adaptive cross approximation of multivariate functions, *Constr. Approx.*, **34** (2011), 149–179.

[5] H.-J. Bungartz and M. Griebel, Sparse grids, *Acta Numer.*, **13** (2004), 147–269.

[6] A. A. Contreras, P. Mycek, O. P. Le Maître, F. Rizzi, B. Debusschere and O. M. Knio, Parallel domain decomposition strategies for stochastic elliptic equations. Part A: Local Karhunen-Loève representations, *SIAM J. Sci. Comput.*, **40** (2018), C520–C546.

[7] A. Damianou and N. Lawrence, Deep Gaussian processes, in *Proceedings of the Sixteenth International Workshop on Artificial Intelligence and Statistics (AISTATS)* (eds. C. Carvalho and P. Ravikumar), AISTATS '13, JMLR W&CP 31, 2013, 207–215.

[8] C. R. Dietrich and G. N. Newsam, Fast and exact simulation of stationary Gaussian processes through circulant embedding of the covariance matrix, *SIAM J. Sci. Comput.*, **18** (1997), 1088–1107.

[9] M. M. Dunlop, M. A. Girolami, A. M. Stuart and A. L. Teckentrup, How deep are deep Gaussian processes?, *J. Mach. Learn. Res.*, **19** (2018), 1–46, URL http://jmlr.org/papers/v19/18-015.html.

[10] M. M. Dunlop, M. A. Iglesias and A. M. Stuart, Hierarchical Bayesian level set inversion, *Statistics and Computing*, **27** (2017), 1555–1584.

[11] M. F. Emzir, S. Lasanen, Z. Purisha and S. Särkkä, Hilbert-space reduced-rank methods for deep gaussian processes, in *2019 IEEE 29th International Workshop on Machine Learning for Signal Processing (MLSP)*, 2019, 1–6.

[12] M. Feischl, F. Y. Kuo and I. H. Sloan, Fast random field generation with H-matrices, *Numer. Math.*, **140** (2018), 639–676.

[13] L. Foster, A. Waagen, N. Aijaz and et al., Stable and efficient Gaussian process calculations, *J. Mach. Learn. Res.*, **10** (2009), 857–882, URL http://www.jmlr.org/papers/v10/foster09a.html.

[14] A. Garriga-Alonso, C. E. Rasmussen and L. Aitchison, Deep convolutional networks as shallow gaussian processes, in *7th International Conference on Learning Representations*, 2019.

[15] M. Gelbrich, On a formula for the L^2 Wasserstein metric between measures on Euclidean and Hilbert spaces, *Math. Nachr.*, **147** (1990), 185–203.

[16] A. L. Gibbs and F. E. Su, On choosing and bounding probability metrics, *Int. Stat. Rev.*, **70** (2002), 419–435.

[17] G. H. Golub and C. F. Van Loan, *Matrix computations*, 4th edition, Johns Hopkins Studies in the Mathematical Sciences, Johns Hopkins University Press, Baltimore, MD, 2013.

[18] I. G. Graham, F. Y. Kuo, D. Nuyens, R. Scheichl and I. H. Sloan, Analysis of circulant embedding methods for sampling stationary random fields, *SIAM J. Numer. Anal.*, **56** (2018), 1871–1895.

[19] N. Halko, P. G. Martinsson and J. A. Tropp, Finding structure with randomness: probabilistic algorithms for constructing approximate matrix decompositions, *SIAM Rev.*, **53** (2011), 217–288.

[20] H. Harbrecht, M. Peters and R. Schneider, On the low-rank approximation by the pivoted Cholesky decomposition, *Appl. Numer. Math.*, **62** (2012), 428–440.

[21] H. Harbrecht, M. Peters and M. Siebenmorgen, Efficient approximation of random fields for numerical applications., *Numer. Linear Algebra Appl.*, **22** (2015), 596–617.
[22] O. Haug, T. L. Thorarinsdottir, S. H. Sørbye and C. L. E. Franzke, Spatial trend analysis of gridded temperature data at varying spatial scales, *arXiv preprint arXiv:1905.13522*.
[23] J. S. Hesthaven, G. Rozza and B. Stamm, *Certified reduced basis methods for parametrized partial differential equations*, SpringerBriefs in Mathematics, Springer, Cham; BCAM Basque Center for Applied Mathematics, Bilbao, 2016.
[24] J. S. Hesthaven, B. Stamm and S. Zhang, Efficient greedy algorithms for high-dimensional parameter spaces with applications to empirical interpolation and reduced basis methods, *ESAIM Math. Model. Numer. Anal.*, **48** (2014), 259–283.
[25] C. F. Higham and D. J. Higham, Deep learning: an introduction for applied mathematicians, *SIAM Review (accepted)*, URL http://eprints.gla.ac.uk/179884/.
[26] N. J. Higham, *Accuracy and stability of numerical algorithms*, 2nd edition, Society for Industrial and Applied Mathematics (SIAM), Philadelphia, PA, 2002.
[27] B. N. Khoromskij, A. Litvinenko and H. G. Matthies, Application of hierarchical matrices for computing the Karhunen-Loève expansion, *Computing*, **84** (2009), 49–67.
[28] U. Khristenko, L. Scarabosio, P. Swierczynski, E. Ullmann and B. Wohlmuth, Analysis of boundary effects on PDE-based sampling of Whittle-Matérn random fields, *SIAM/ASA J. Uncertain. Quantif.*, **7** (2019), 948–974.
[29] J. Latz, M. Eisenberger and E. Ullmann, Fast sampling of parameterised Gaussian random fields, *Comput. Methods Appl. Mech. Engrg.*, **348** (2019), 978–1012.
[30] F. Lindgren, H. v. Rue and J. Lindström, An explicit link between Gaussian fields and Gaussian Markov random fields: the stochastic partial differential equation approach, *J. R. Stat. Soc. Ser. B Stat. Methodol.*, **73** (2011), 423–498.
[31] S. L. Lohr, *Sampling: design and analysis*, 2nd edition, Brooks/Cole, Cengage Learning, Boston, MA, 2010.
[32] V. Minden, A. Damle, K. L. Ho and L. Ying, Fast spatial Gaussian process maximum likelihood estimation via skeletonization factorizations, *Multiscale Model. Simul.*, **15** (2017), 1584–1611.
[33] A. Nouy, A priori model reduction through proper generalized decomposition for solving time-dependent partial differential equations, *Comput. Methods Appl. Mech. Engrg.*, **199** (2010), 1603–1626.
[34] C. E. Rasmussen and C. K. I. Williams, *Gaussian Processes for Machine Learning*, The MIT Press, 2006.
[35] A. K. Saibaba, J. Lee and P. K. Kitanidis, Randomized algorithms for generalized Hermitian eigenvalue problems with application to computing Karhunen-Loève expansion., *Numer. Linear Algebra Appl.*, **23** (2016), 314–339.
[36] F. Schäfer, T. J. Sullivan and H. Owhadi, Compression, inversion, and approximate PCA of dense kernel matrices at near-linear computational complexity, *arXiv preprint arXiv:1706.02205*.
[37] C. Schwab and R. A. Todor, Karhunen-Loève approximation of random fields by generalized fast multipole methods, *J. Comput. Phys.*, **217** (2006), 100–122.
[38] I. Sraj, O. P. Le Maître, O. M. Knio and I. Hoteit, Coordinate transformation and polynomial chaos for the Bayesian inference of a Gaussian process with parametrized prior covariance function, *Comput. Methods Appl. Mech. Engrg.*, **298** (2016), 205–228.
[39] M. L. Stein, *Interpolation of Spatial Data*, Springer-Verlag, New York, 1999.
[40] A. M. Stuart and A. L. Teckentrup, Posterior consistency for Gaussian process approximations of Bayesian posterior distributions, *Math. Comp.*, **87** (2018), 721–753.
[41] A. Townsend, *Computing with functions in two dimensions*, ProQuest LLC, Ann Arbor, MI, 2014, URL http://gateway.proquest.com/openurl?url_ver=Z39.88-2004&rft_val_fmt=info:ofi/fmt:kev:mtx:dissertation&res_dat=xri:p Thesis (D.Phil.)–University of Oxford (United Kingdom).
[42] A. Townsend and L. N. Trefethen, An extension of Chebfun to two dimensions, *SIAM J. Sci. Comput.*, **35** (2013), C495–C518.
[43] A. Townsend and L. N. Trefethen, Continuous analogues of matrix factorizations, *Proc. A.*, **471** (2015), 20140585, 21.
[44] C. Villani, *Optimal transport*, vol. 338 of Grundlehren der Mathematischen Wissenschaften [Fundamental Principles of Mathematical Sciences], Springer-Verlag, Berlin, 2009.

[45] C. K. Wikle, Hierarchical models for uncertainty quantification: An overview, in *Handbook of Uncertainty Quantification* (eds. R. Ghanem, D. Higdon and H. Owhadi), Springer International Publishing, Cham, 2016, 1–26.

[46] C. K. Williams and M. Seeger, Using the Nyström method to speed up kernel machines, in *Advances in neural information processing systems*, 2001, 682–688, URL http://papers.nips.cc/paper/1866-using-the-nystrom-method-to-speed-up-kernel-machines.pdf.

Received xxxx 20xx; revised xxxx 20xx.

E-mail address: daniel.kressner@epfl.ch
E-mail address: jl2160@cam.ac.uk
E-mail address: s.massei@tue.nl
E-mail address: elisabeth.ullmann@ma.tum.de